

# Layer-by-Layer Self-Assembly of Glucose Oxidase with a Poly(allylamine)ferrocene Redox Mediator

Jose Hodak, Roberto Etchenique, and Ernesto J. Calvo\*,†

INQUIMAE, Facultad de Ciencias Exactas y Naturales, Pabellon 2, Ciudad Universitaria, AR-1428 Buenos Aires, Argentina

Kavita Singhal and Philip N. Bartlett

Department of Chemistry, University of Southampton, Highfield, Southampton, SO17 1BJ, United Kingdom

Received November 18, 1996. In Final Form: February 27, 1997

We report the redox mediation of glucose oxidase (GOx) in a self-assembled structure of cationic poly(allylamine) modified by ferrocene (PAA-Fc) and anionic GOx deposited electrostatically layer-by-layer on negatively charged alkanethiol-modified Au surfaces. Successive PAA-Fc and GOx layers were deposited by alternate immersion of the thiol-modified Au in the respective polyelectrolyte and enzyme solutions. The uptake of thiol, redox polymer, and GOx on the surface was monitored by quartz crystal microbalance. Cyclic voltammetry shows nearly ideal surface waves of ferrocene in the polymer with charge independent of sweep rate; the redox surface concentration was obtained from integration of the ferrocene/ferricinium voltammetric peaks. The redox charge increases in step with the number of PAA-Fc layers deposited. Enzyme catalysis for the oxidation of  $\beta$ -D-glucose was achieved with a multilayer PAA-Fc/GOx assembly, with each GOx layer contributing equally to the catalytic response. Only a small fraction of the active assembled GOx molecules are "electrically wired" by the ferrocene polymer although all of the enzyme could be oxidized by soluble ferrocenesulfonate when added to solution.

## Introduction

Molecular level design of integrated chemical systems has received considerable attention in recent years.<sup>1</sup> The formation of such systems which facilitate directional electron transfer has proved invaluable to the advancement of biosensor and molecular device technologies. An integrated chemical system can be viewed as the controlled assembly of several chemical components resulting in a system which functions efficiently and effectively as specified by the designer. The inclusion of a biological component, such as an enzyme, has increased the applicability of integrated chemical systems to biosensor technology. By integration of an enzyme and/or mediator on to a transducing component, generally an electrode, further applications in the field of molecular devices can be envisaged.<sup>2</sup> The integrated chemical system described here involves the formation of a structure consisting of alternating layers of redox polymer and enzyme. The structure is built up on a thiol-modified gold surface through electrostatic interactions between the layers, and the electrochemical and catalytic responses are proportional to the number of layers present. In previous communications<sup>3</sup> we have reported hydrogels of poly(allylamine) (PAA) modified with redox groups and cross-linked with glucose oxidase (GOx). In that work negatively charged GOx and polycationic PAA were first associated electrostatically, and then the NH<sub>2</sub> groups of the PAA were cross-linked with the terminal NH<sub>2</sub> groups of surface lysine residues of the enzyme. Redox hydrogels of this type not only provide a very suitable environment for

enzyme entrapment but also allow electrochemical oxidation of the redox prosthetic FAD group of GOx and the electrode by a diffusion-like electron-hopping mechanism mediated by the redox groups attached to the polymer backbone.<sup>4</sup> Charge propagation in PAA gels was further investigated by electrochemical modulation of the fluorescence of covalently attached flavin moieties.<sup>5</sup>

Heller has shown that polycationic redox polymers adsorbed on graphite can strongly bind the enzyme glucose oxidase (GOx) and that the bound enzyme can then be electrochemically oxidized by the base electrode through mediation by the redox polymer, so-called "molecular wiring" of the enzyme.<sup>6</sup> Subsequent papers have described the catalytic oxidation of glucose in two- and three-dimensional structures in which GOx is "molecularly wired" by the redox polymer.<sup>7</sup> This use of redox hydrogels provides a modified electrode layer in which the mediator and enzyme are coimmobilized; however this approach does not allow controlled monolayer deposition of polymer and/or enzyme.

An alternative approach is to use self-assembly to build-up active enzyme monolayers at the electrode surface, and there are several examples of related systems in the literature. These include not only those based on thiol-modified electrodes but also structures based on Langmuir–Blodgett films,<sup>8</sup> biotin/avidin interactions,<sup>9</sup> or immunological binding between antibody and antigen molecules.<sup>10</sup> For example, Willner *et al.*<sup>11,12</sup> have dem-

\* Corresponding author.

† Permanent Research Fellow of the Argentine Research Council (CONICET).

© Abstract published in *Advance ACS Abstracts*, April 1, 1997.

(1) Bard, A. J. *Integrated Chemical Systems, A Chemical Approach to Nanotechnology*; J. Wiley & Sons: New York, 1994.

(2) Bartlett, P. N.; Birkin, P. R. *Anal. Chem.* **1993**, *65*, 1118–1119. Bartlett, P. N.; Birkin, P. R. *Anal. Chem.* **1994**, *66*, 1552–1559.

(3) Calvo, E. J.; C. Danilowicz, C.; Diaz, L. *J. Electroanal. Chem.* **1994**, *369*, 279–282.

(4) Danilowicz, C.; Etchenique, R.; Calvo, E.; Diaz, L. *J. Anal. Chem.* **1996**, *68*, 4186–4193.

(5) Bonazzola, C.; Brust, M.; Calvo, E. J. *J. Electroanal. Chem.* **1996**, *407*, 203–207.

(6) Heller, A. *Acc. Chem. Res.* **1992**, *23*, 128–134.

(7) Heller, A. *J. Phys. Chem.* **1992**, *96*, 3579–3587.

(8) Sun, S.; Ho-Si, P. H.; Harrison, D. J. *Langmuir* **1991**, *7*, 727–737.

(9) Hoshi, T.; Anzai, J.; Osa, T. *Anal. Chem.* **1995**, *67*, 770–774.

(10) Bourdillon, C.; Demaille, C.; Moiroux, J.; Saveant, J. M. *J. Am. Chem. Soc.* **1994**, *116*, 10328–10329.

(11) Willner, J.; Riklin, A.; Shoham, B.; Rivenzon, D.; Katz, E. *Adv. Mater.* **1993**, *5*, 912–915.

(12) Willner, J.; Katz, E. *Anal. Chem.* **1994**, *66*, 1535–1539.

onstrated the formation of up to four layers of ferrocene-modified GOx on a thiol layer. The resulting catalytic response for glucose was found to be proportional to the number of layers present.

The approach we report here uses a gold electrode modified by a thiol layer with negatively charged end groups on which we electrostatically build layers of a positively charged redox polymer, poly(allylamine) (PAA) with ferrocene redox sites (Fc) attached along the backbone, and polyanionic GOx. With this technique we can produce multilayered structures in which enzyme mediation is provided by the ferrocene sites on the polymer; that is, the system is self-contained and does not rely on the addition of a mediator to the solution or covalent modification of the enzyme.

Bartlett and Pratt<sup>13</sup> have presented a comprehensive treatment of diffusion and reaction within a uniform film containing immobilized enzyme and mediator at an electrode surface. This model describes the effects of film thickness, substrate, enzyme and mediator concentrations, and electrode potential on the catalytic current. Using this type of model we are able to analyze the catalytic responses of our multilayer films as a function of the applied potential, the glucose concentration, and the number of enzyme layers.

The idea of using thiol modification of gold to produce an anionic surface for adsorption of polycations has been described before. Electrostatic binding between a carboxylate-terminated thiol and polycationic poly(L-lysine) was demonstrated by Corn *et al.*<sup>14</sup> Mizutani *et al.*<sup>15</sup> then extended this idea and coadsorbed GOx with poly(L-lysine) on a monolayer of mercaptopropionic acid. The oxidation current for hydrogen peroxide at the gold electrode, resulting from the enzyme-catalyzed reaction between glucose and oxygen, was then related to the concentration of glucose in solution.

In this case we use PAA as our polycation. Small angle X-ray scattering of PAA hydrochloride has shown the ordered arrangement of the macroions in solution.<sup>16</sup> In addition, Decher and co-workers<sup>17</sup> have recently shown that PAA can be used to form ultrathin films by electrostatic attraction of macromolecules of opposite charge. Alternating adsorption of anionic and cationic polyelectrolytes was employed for the formation of multilayer assemblies of DNA/PAA,<sup>18</sup> poly(vinylsulfonate)/PAA,<sup>19</sup> and poly(styrenesulfonate)/PAA.<sup>20</sup> In this strategy the strong electrostatic interactions between polyanion and polycation are the driving force for multilayer self-assembly, and uniform molecular films of well-defined thickness are formed. This thickness increases linearly with the number of layers in the repeating ABAB... multilayer. The relatively high concentration of polyelectrolyte in the adsorption solution results in an excess of ionic charge exposed to the solution, due to the effects of screening, and thus the surface charge is reversed in each layer. In a related study using inorganic systems Mallouk described

the increase in thickness, as determined by ellipsometry, in the layer-by-layer assembly of intercalated PAA with anionic  $\alpha$ -Zr(HPO<sub>4</sub>)<sub>2</sub>( $\alpha$ -ZrP).<sup>21</sup>

This type of approach has been used to immobilize enzymes. Lvov and Kunitake<sup>20b</sup> have reported the layer-by-layer adsorption of GOx and PEI (polyethylenimine). They were able to follow the multilayer formation using the quartz crystal microbalance and found a linear growth of the film up to 25 molecular layers. However in this case no attempt was made to measure the activity of the immobilized enzyme and polymers employed were not redox active and therefore could not act as mediators for electrochemical oxidation of the enzyme.

Quartz crystal microgravimetry (QCM) has also been used recently to follow quantitatively the self-assembly of nanometer-sized Au and CdS particles in multilayer structures of dithiol-derivatized Au formed on surfaces.<sup>22</sup>

In the present work we have investigated for the first time as proof-of-concept the successive alternate deposition of Fc-PAA and GOx layers on an Au surface initially thiolated with negatively charged sulfonic groups. We have studied the propagation of charge within the resulting structures and the enzyme catalysis using both electrochemical methods and *in situ* quartz crystal microgravimetry with quartz crystal impedance measurements.

## Experimental Section

In the course of experiments the following chemicals were used as supplied: sodium 2-mercaptoacetate (Aldrich), sodium 3-mercapto-1-propanesulfonate (Aldrich), ferrocene carboxaldehyde (Aldrich), high molecular weight poly(allylamine)hydrochloride (Aldrich); sodium borohydride (Riedel-de-Haën); glucose (Merck). Glucose oxidase, GOx (EC 1.1.3.4 type VII-S from *Aspergillus niger*, 186 kDa, 250 mg mL<sup>-1</sup>) was a gift from MediSense, UK.

Poly(allylamine) was dialyzed against water for 80 h using a D-9652 Sigma dialysis membrane (molar mass cutoff 12 000) in order to eliminate low molecular weight oligomers; the solution was then freeze-dried. Glucose solutions were prepared from a stock solution equilibrated in the anomers, and kinetics herein refer to the total glucose concentration. All solutions were prepared in milli-Q (Millipore) water and stored at 4 °C.

**Synthesis of Ferrocene Poly(allylamine).** Ferrocene carboxaldehyde (8 mg) was dissolved in 5 cm<sup>3</sup> methanol and added dropwise within an hour to 30 cm<sup>3</sup> of anhydrous methanolic solution of 40 mg of poly(allylamine) containing 0.26 cm<sup>3</sup> of triethylamine. The mixture was stirred for another hour at room temperature, sodium borohydride was carefully added in portions at 0 °C, and stirring continued for 90 min; finally the mixture was dried *in vacuo* at 35 °C and the residue was extracted with distilled water. The aqueous solution was further purified by membrane dialysis against water.

Total iron content in the PAA polymer was determined spectrophotometrically at 440 nm using a calibration curve for ferrocene in methanol ( $\epsilon_{440} = 84 \text{ M}^{-1} \text{ cm}^{-1}$ ).

**Electrochemical Experiments.** Gold flags (50–60 mm<sup>2</sup>) used as working electrodes were cleaned by polishing thoroughly with 0.3  $\mu\text{m}$  alumina, sonicating for a few minutes, and then placing in fresh piranha solution (1:3 H<sub>2</sub>O<sub>2</sub>/98% H<sub>2</sub>SO<sub>4</sub>) for 20 min. **Caution Piranha solution is highly corrosive and reacts violently with organic materials: suitable precautions must be taken at all times.** Used thiol-modified electrodes were cleaned by immersion in hot 1:1 nitric/sulfuric acid for 3 h and further short immersion in aqua regia. Clean electrodes were rinsed with Milli-Q water and used immediately after cleaning. Before thiol adsorption the electrodes were cycled in 2 M sulfuric acid between 0 and 1.7 V at 0.1 V s<sup>-1</sup> to check for surface contamination.<sup>23</sup>

(21) Keller, S. W.; Kim, H.; Mallouk, T. E. *J. Am. Chem. Soc.* **1994**, *116*, 8817–8818.

(22) Brust, M.; Etchenique, R.; Calvo, E. J.; Gordillo, G. *J. Chem. Soc., Chem. Commun.* **1996**, 1949–1950.

(23) Angerstein-Kozłowska, H.; Conway, B. E.; Barnett, B.; Mozzota, J. *J. Electroanal. Chem.* **1979**, *100*, 417–446.

(13) Bartlett, P. N.; Pratt, K. F. E. *J. Electroanal. Chem.* **1995**, *397*, 61–78.

(14) Jordan, C. E.; Frey, B. L.; Kornguth, S.; Corn, R. M. *Langmuir* **1994**, *10*, 3642–3648.

(15) Mizutani, F.; Sato, Y.; Yabuki, S.; Hirata, Y. *Chem. Lett.* **1996**, *251*, 252.

(16) Yoshikawa, Y.; Matsuoka, H.; Ise, N. *Br. Polym. J.* **1986**, *18*, 242–246.

(17) Decher, G.; Hong, J. D. *Ber. Bunsenges. Phys. Chem.* **1991**, *95*, 1430.

(18) Lvov, Y.; Decher, G.; Sukhorukov, G. *Macromolecules* **1993**, *26*, 5396–5399.

(19) Lvov, Y.; Decher, G.; Mohwald, H. *Langmuir* **1993**, *9*, 481–486.

(20) (a) Decher, G.; Hong, J. D.; Schmitt, J. *Thin Solid Films* **1992**, *210/211*, 831–835. (b) Lvov, Y.; Ariga, K.; Ichinose, I.; Kunitake, T. *J. Am. Chem. Soc.* **1995**, *117*, 6117–6123.

A standard three-electrode electrochemical cell was employed with an operational amplifier potentiostat. A platinum auxiliary electrode and saturated calomel reference (SCE) were employed. All potentials herein are quoted with respect to this reference.

**Quartz Crystal Microbalance Experiments.** A modified Pierce-Miller transistor oscillator was used<sup>24</sup> with the resonant circuit placed in a stainless steel case at the bottom of the balance which provides both the Faraday cage and fixed and short fixtures. The frequency was measured with a HP5334B frequency meter connected to an AT-386 PC via an IEEE-488 interface, with a 0.1 Hz resolution and a stability better than 1 Hz/min. Data acquisition software was written in Quick BASIC 4.5 and this controlled the electrode potential with respect to the reference electrode and the rf signal with respect to the Au back-plate of the quartz crystal.<sup>24</sup>

Quartz crystal impedance measurements were performed with a fast technique based on a 10 MHz ac-voltage divider formed by the quartz crystal and a measuring impedance,  $Z_m$ .<sup>24</sup> A nonlinear fit of the complex ratio of the output ac voltage to the input ac voltage, to the Butterworth-Van Dyke (BVD) equivalent circuit equation yields the quartz crystal impedance parameters  $X_L (= \omega L)$  and  $R^2$ .<sup>24</sup>

Overtone polished 10 MHz AT-cut quartz crystals (20 mm diameter, 0.167 mm thickness, Kristall-Verarbeitung Neckar-bischofsheim GmbH, cat. XA 1600, Germany) with an active area of 1.77 cm<sup>2</sup> were employed. After oxygen reactive sputtering 2 nm Cr and 200 nm Au were deposited. For quartz impedance measurements 14 mm diameter, 0.168 mm thick quartz crystals (ICM, Oklahoma City, OK, cat. 31210) were used with an active area of 0.196 cm<sup>2</sup> and with 100 nm of Au deposit. The crystals were mounted in the cell by means of sealing O-rings with only one face in contact with the electrolyte; this face was a common ground to both the ac and dc circuits.

**The Self-Assembly Process.** The adsorption times for each component, thiol, polymer, and enzyme, were determined by a preliminary QCM study. In these experiments all solutions and the QCM cell were allowed to reach thermal equilibrium before mixing in order to avoid any frequency shifts caused by changes of temperature.

**Thiol Adsorption.** Thiol solutions were freshly prepared before each adsorption experiment in order to avoid oxidation in air. The thiol monolayer was formed by soaking Au electrodes in aqueous solutions of 0.02 M sodium 3-mercapto-1-propane-sulfonate in 0.01 M H<sub>2</sub>SO<sub>4</sub> for 2 h. The Au samples were removed from the adsorption solution, thoroughly washed in distilled water, and stored in water.

**PAA-Fc Adsorption.** The poly(allylamine)ferrocene derivative was adsorbed from 0.020 to 0.035 mM (monomer referred to monomer molar mass) aqueous solutions for 30–40 min. After adsorption the modified electrodes were thoroughly rinsed with distilled water and stored in 10 mM, pH 5 acetate buffer at 4 °C.

**GOx Adsorption.** Glucose oxidase was adsorbed onto the PAA-Fc modified Au from an aqueous solution containing 7  $\mu$ M enzyme in 10 mM, pH 5 acetate buffer over 20–25 min. After being rinsed with distilled water the electrodes were stored in 10 mM, pH 5 acetate buffer at 4 °C.

In EQCM experiments the same adsorption routine was followed, except that 100  $\mu$ L of a more concentrated enzyme solution (67  $\mu$ M or 12.5 mg mL<sup>-1</sup>) was used. The enzyme solution was added to 1 cm<sup>3</sup> of stirred buffer which was in contact with the quartz crystal. Mechanical stirring was continued in order to avoid disturbances due to the mixing of the solutions. Addition of further solutions proved that adsorption equilibrium was reached and that no hydrodynamic disturbances were observed.

Enzyme catalysis experiments were carried out under a N<sub>2</sub> atmosphere with stirring in background buffer electrolyte. Small additions of glucose from a stock solution were made by means of automatic micropipets (Eppendorf Varipette 4710).

## Results and Discussion

The alternate adsorption of the polycationic PAA-Fc and polyanionic GOx is schematically depicted in Figure 1. The first step in building up the structure is the

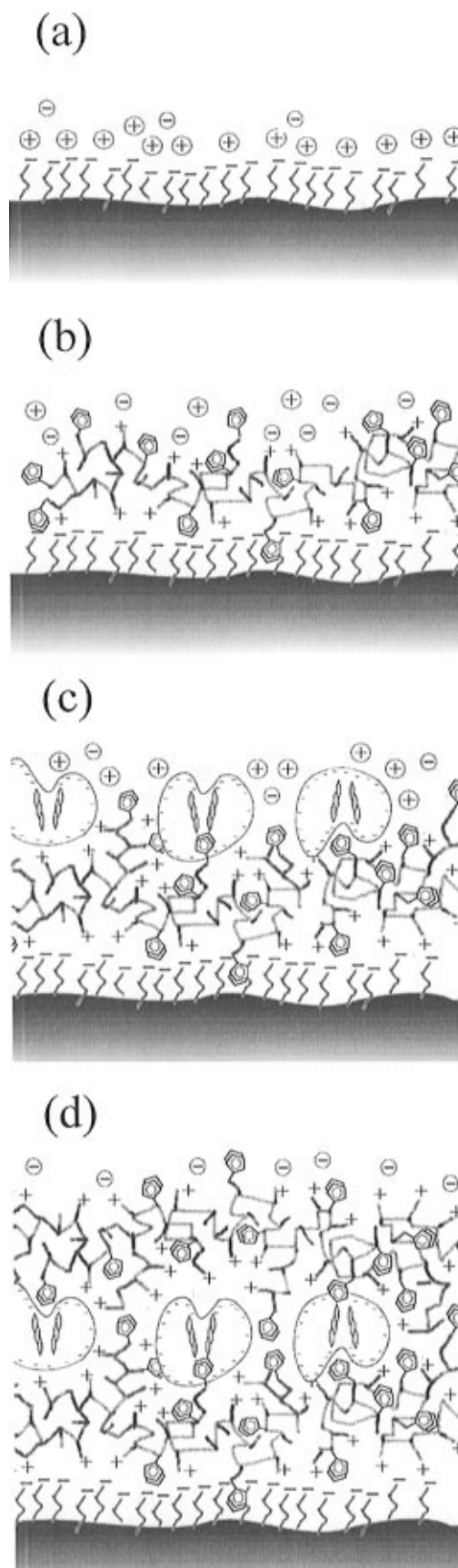


**Figure 1.** Idealized schematic representation of the alternate self-assembled (SA) multilayer buildup: (a) thiol adsorption on Au; (b) PAA-Fc adsorption; (c) GOx adsorption; (d) alternate PAA-Fc/GOx/PAA-Fc layers.

adsorption of thiol on Au to produce a negatively charged surface (Figure 1a). The second step is then the adsorption

(24) Calvo, E. J.; Danilowicz, C.; Etchenique, R. *J. Chem. Soc., Faraday Trans.* **1995**, *91*, 4083–4091.

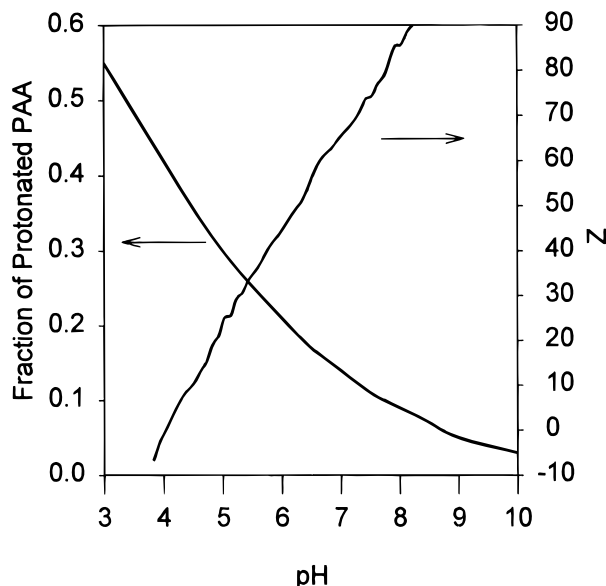


**Figure 2.** Fraction of protonated poly(allylamine) in solution (ref 16) and average charge on glucose oxidase (ref 27) as a function of pH (experimental data replotted from refs 16 and 27).

of the ferrocene derivatized polycation leaving a net positive charge on the surface (Figure 1b). GOx is then adsorbed reversing the net charge on the surface so that a negative charge is now exposed to the solution (Figure 1c). By repetition of the sequence of polymer and enzyme adsorption steps, a multilayer structure can be built up (Figure 1d).

The electrostatic interaction between  $\text{PAA}^{n+}$  and  $\text{GOx}^{m-}$  is strongly influenced by the electrolyte concentration and by the solution pH, and it is therefore important to select the correct pH to achieve this layer by layer assembly. The isoelectric point of native GOx is 4.05<sup>25</sup> so that above this pH the enzyme carries a net negative charge which increases with the solution pH, as shown in Figure 2. Titration of the amine groups in PAA<sup>16,26</sup> shows that the free energy of protonation depends on the pH and yields a smooth transition from fully protonated to fully unprotonated polymer as the pH of the solution increases. A plot of the fraction of protonated PAA as a function of pH using experimental data from the literature<sup>16</sup> is also shown in Figure 2. The choice of pH for layer-by-layer self-assembly is therefore a compromise between the requirements of the polymer and those of the enzyme. In addition the enzyme activity is also pH dependent, and this must also be taken into account. We therefore chose to work at pH 5. At pH 5 30% of the amine groups in the PAA are protonated so that the polymer carries a net positive charge, at the same pH GOx has a net negative charge of -24, and the enzyme is active for glucose oxidation.

**Thiol Adsorption.** Preliminary experiments with thioacetate as well as mercaptopropenesulfonate showed that these thiols promote the electrostatic adsorption of ferrocene-modified poly(allylamine) on gold at pH 5. Thioacetate,  $\text{p}K_a = 3.68$ ,<sup>27</sup> is fully deprotonated at pH 5 and adsorption of PAA takes place as shown by the redox wave of ferrocene (when transferred to polymer-free

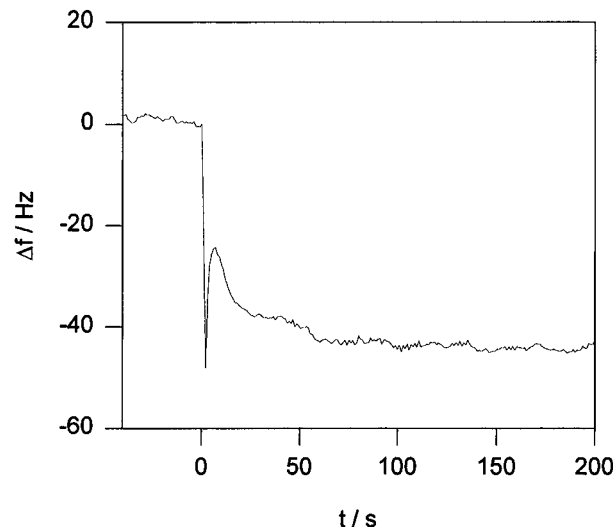


**Figure 3.** Time dependence of the quartz crystal resonance frequency shift for the adsorption of 3-mercaptopropenesulfonate on Au from 0.02 mM thiol solution in 0.01 M  $\text{H}_2\text{SO}_4$ . Measurements were made using a 10 MHz AT-cut quartz crystal with an areal mass sensitivity of  $0.229 \text{ Hz cm}^2 \text{ ng}^{-1}$ .

electrolyte). The peak width at half peak height (fwhh) for the ferrocene oxidation is 140 mV and is thus larger than that expected for an ideal surface wave,  $90.6/n \text{ mV}$ . This suggests the existence of repulsive interactions<sup>28</sup> or a distribution of redox formal potentials.<sup>29</sup>

The concentration of 2-mercaptoacetate present in the anionic form is itself dependent on the solution pH, and for this reason mercaptopropenesulfonate, which is the salt of a much stronger acid and thereby fully ionized at pH 5, was preferred. Mercaptopropenesulfonate modification of the Au electrodes produced a stable layer of PAA-Fc with much more reversible electrochemistry.

Typical results for 3-mercaptopropenesulfonate adsorption on Au obtained with the quartz crystal microbalance (QCM) are depicted in Figure 3. For a 10 MHz quartz crystal according to the Sauerbrey equation the decrease of frequency,  $\Delta f$ , corresponds to an increase of mass,  $\Delta m$ , due to the uptake of thiol by the surface<sup>30</sup>

$$\Delta f = - \frac{2f_0^2}{\sqrt{\mu_Q \rho_Q}} \frac{\Delta m}{A} \quad (1)$$

where  $f_0$  is the resonant frequency of the AT-quartz crystal,  $\rho_Q = 2650 \text{ kg m}^{-3}$  is the density of quartz,  $\mu_Q = 2.957 \times 10^{-10} \text{ N m}^{-2}$  is the elastic coefficient of quartz, and  $\Delta m/A$  is the areal mass density of the deposit.

On addition of the thiol to the solution the frequency decreases corresponding to an increase in mass. The initial sharp spike is due to mixing effects in the solution and is followed by a slow uptake of thiol over about 100 s. The frequency shift due to changes of viscosity and density upon addition of thiol in this experiment is negligible (less than 1 Hz). This was demonstrated by making a separate addition of thiol in to background electrolyte solution in contact with the thiolated Au-coated quartz crystal following the same protocol as that used in the original experiment.

The time course of this adsorption is similar to that for the adsorption of long chain alkanethiols reported by

(25) Voet, J. G.; Coe, J.; Epstein, J.; Matossian, V.; Shipley, T. *Biochemistry* **1981**, 20, 7182–7185.

(26) Suh, J.; Paik, H.; Hwang, B. K. *Bioorg. Chem.* **1994**, 22, 318–327.

(27) Dawson, R. M. C.; Elliot, D. C.; Elliot, W. H.; Jones, K. M. *Data for Biochemical Research*, 3rd ed.; Oxford University Press: Oxford, 1986.

(28) Murray R. W. In *Molecular Design of Electrode Surfaces*; Murray, R. W., Ed.; John Wiley & Sons: New York, 1992; p 1.

(29) Nahir, Tal M.; Bowden, E. F. J. *Electroanal. Chem.* **1996**, 410, 9–13.

(30) Sauerbrey, G. *Z. Phys.* **1959**, 155, 206–222.

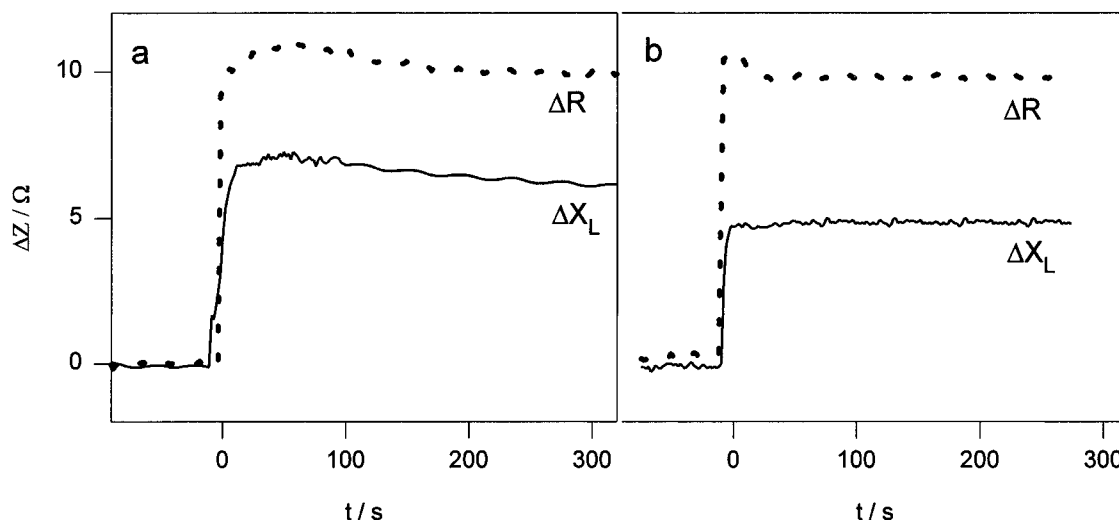


**Figure 4.** *In situ* quartz crystal impedance ( $\Delta X_L$  and  $\Delta R$ ) for the adsorption of PAA-Fc on thiol-modified Au (a) and for the addition of 0.2 mL of 70 mM PAA-Fc in 0.2 mL of distilled water on previously adsorbed PAA-Fc (b).

Doblhofer.<sup>31</sup> The amount of thiol adsorbed can be obtained by substitution of the observed frequency shift in eq 1. This gives a calculated mass increase of  $174 \text{ ng cm}^{-2}$  which corresponds to  $0.98 \text{ nmol cm}^{-2}$  of sodium 3-mercapto-1-propane sulfonate (relative molar mass  $178 \text{ g mol}^{-1}$ ). This is comparable to the value reported for octadecanethiol<sup>31</sup> ( $0.93 \text{ nmol cm}^{-2}$ ).

**Polymer Adsorption.** The use of the QCM technique to measure polymer uptake by electrostatic adsorption onto the mercaptopropanesulfonate surface is complicated by a strong viscoelastic effect due to the rheological properties of the PAA solutions. Using the Pierce-Miller oscillator, which operates at the parallel resonant frequency,<sup>24</sup> we observe a positive frequency shift upon addition of PAA solution. This result cannot be explained by either a simple mass change or an increase in the Newtonian viscosity of the solution.

To overcome this problem, we made use of quartz crystal impedance analysis<sup>24</sup> which allows us to follow the change in reactance,  $\Delta X_L$ , and viscous resistive,  $\Delta R$ , components of the response as adsorption proceeds. On addition of PAA-Fc to the buffer solution in contact with the thiol-modified gold-coated quartz crystal both,  $\Delta X_L$  and  $\Delta R$  increase, Figure 4a. When the quartz crystal was then removed from the PAA-Fc solution and thoroughly rinsed with water, electrochemical measurements show that PAA-Fc was present on the surface (*vide infra*). Measurements of the quartz impedance parameters for the modified quartz crystal in water give changes in  $\Delta X_L$  and  $\Delta R$  of 1.6 and 0.2  $\Omega$ , respectively, when compared to the corresponding values for the crystal in water before adsorption of the PAA-Fc. From this we conclude that the abnormal increase in  $\Delta X_L$  and  $\Delta R$  with  $\Delta R > \Delta X_L$  seen in Figure 4a is entirely due to the rheological properties of the polymer solution in contact with the quartz crystal, and from the data in Figure 4b we obtain the viscoelastic parameters: viscous loss modulus,  $G'' = 6.1 \times 10^4 \text{ N m}^{-2}$  and elastic storage modulus,  $G' = 1.3 \times 10^3 \text{ N m}^{-2}$  for 35 mM PAA-Fc aqueous solution at 10 MHz.

Confirmation of this interpretation is obtained by repeating the experiment with addition of PAA-Fc to water but now using the crystal which was already coated with PAA-Fc. Then we expect to see the same rheological changes in the solution but no further PAA-Fc adsorption on to the crystal. Figure 4b shows the results for this

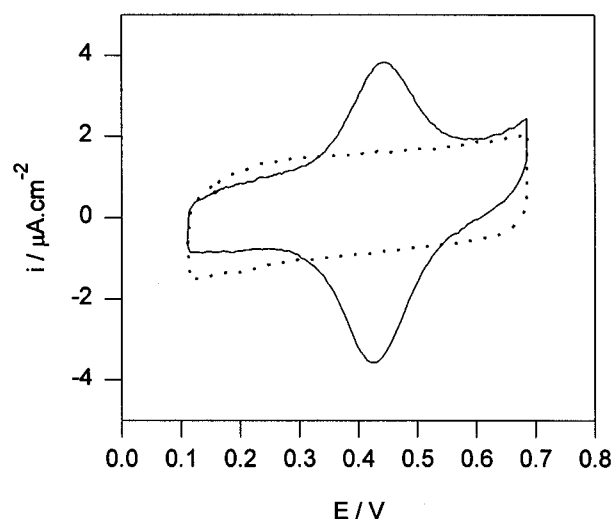


**Figure 5.** Cyclic voltammogram of Au with 3-mercapto-1-propanesulfonate SAM (···) and Au/Thiol with Fc-PAA SAM in 10 mM acetic/acetate buffer of pH 5.0 (—). Sweep rate:  $50 \text{ mV s}^{-1}$ . (a) Au/thiol; (b) Au/thiol/PAA-Fc. Ferrocene charge:  $6.5 \mu\text{C cm}^{-2}$ .

experiment. On addition of PAA-Fc to the water,  $\Delta R$  increases in approximately the same manner and by the same amount as in the first experiment (compare to Figure 4a). In contrast  $\Delta X_L$  increases but by a lesser amount than in the first experiment (again compare with Figure 4a). This agrees with our interpretation, and by comparison of the two steady state values of  $\Delta X_L$  we can obtain an estimate of the mass of adsorbed PAA-Fc. Comparison of the  $\Delta X_L$  transients in Figure 4 indicates that a change of approximately 1  $\Omega$  arises from the mass increase. This is equivalent to  $46 \text{ ng cm}^{-2}$  or  $0.49 \text{ nmol cm}^{-2}$  of monomer units on the surface (based on a mean relative molar mass for PAA-Fc-acetate of  $94 \text{ g mol}^{-1}$ ). This corresponds to one-half the surface concentration of thiolsulfonate groups ( $0.98 \text{ nmol cm}^{-2}$ ).

Figure 5 shows a comparison of cyclic voltammograms of Au/thiol and Au/thiol/PAA-Fc modified electrodes in 10 mM acetate buffer. The thiol-modified Au shows only capacitive current over the range 0.1–0.7 V corresponding to a capacitance of  $25 \mu\text{F cm}^{-2}$ . Following adsorption of the redox polymer, typical ferrocene/ferricinium surface redox waves are observed with a small peak separation (ca. 28 mV at  $0.05 \text{ V s}^{-1}$ ) and full width at half peak height of 115 mV (somewhat larger than  $90.6/n \text{ mV}$  for an

(31) Frubose, C.; Doblhofer, K. *J. Chem. Soc., Faraday Trans.* **1995**, *91*, 1949–1953.

ideal surface wave<sup>28</sup>). A linear increase of the peak current with sweep rate was observed which corresponds to the oxidation and reduction of a constant amount of immobilized ferrocene on the time scale of the voltammetry (sweep rates from 5 to 500 mV s<sup>-1</sup>). A decrease in the capacitance, from 25 to 17  $\mu\text{F cm}^{-2}$  is also observed following polymer adsorption. This is consistent with the surface layer becoming more densely packed on adsorption of the redox polymer. The observed surface electrochemistry of the ferrocene shows that the short chain alkanethiols are flexible enough to allow random coil diffusion of redox groups in PAA to approach the gold surface closely enough for electron transfer to occur at an appreciable rate.

The charge involved in the surface process was estimated by integration of the voltammetric peaks. This calculation gave 4–5  $\mu\text{C cm}^{-2}$  from which a ferrocene surface coverage of  $(4-5) \times 10^{-11} \text{ mol cm}^{-2}$  was calculated. We can compare this to the value we calculate from the QCM data. From those experiments we obtained a coverage of 0.49 nmol cm<sup>-2</sup> of monomer units. Chemical analysis of the polymer shows that on average there is one ferrocene unit for every 10 monomer units<sup>3</sup> so that we would expect a ferrocene coverage, from the QCM data, of 0.049 nmol cm<sup>-2</sup>, a value which agrees well with the result of the independent electrochemical measurement.

Further support for the idea that electrostatic interactions play an important part in the adsorption was provided by blank experiments in which no PAA adsorption was observed at bare Au. Similarly attempts to adsorb PAA-Fc to a cystamine modified Au resulted in no evidence of PAA-Fc adsorption. Self-assembled cystamine at pH 5 has positively charged terminal  $\text{NH}_3^+$  and hence it is not expected to promote electrostatic adsorption of PAA-Fc.<sup>32</sup>

**Enzyme Adsorption.** Electrostatic adsorption of polyanionic GOx on the poly(allylamine) top layer is shown by the large negative frequency shift observed by the QCM. To characterize this process we again use quartz crystal impedance measurements. Figure 6 shows the time evolution of  $\Delta X_L$  and  $\Delta R$  following the addition of GOx solution to the Au/Thiol/PAA-Fc surface in contact with buffer. Immediately following the addition of GOx to the solution,  $\Delta X_L$  rapidly increases to a maximum value before falling back to a steady state over about 400 s. The corresponding viscous resistance,  $\Delta R$ , follows the initial peak in  $\Delta X_L$ . This indicates that in the early stages of adsorption of GOx onto the PAA-Fc surface there are significant viscoelastic changes which make a simple interpretation of the mass uptake impossible. However at long times we find that  $\Delta R$  goes to zero so that in the steady state  $\Delta X_L$  can be used to give a measure of the mass uptake. Under these circumstances the Sauerbrey approximation applies and<sup>24</sup>

$$\Delta X_L = \omega \Delta L_m = \frac{2\omega_0^2 L_Q}{\pi \sqrt{\rho_Q \mu_Q}} \frac{\Delta m}{A} \quad (2)$$

with  $L_Q \approx 7.49 \times 10^{-3} \text{ H}$  and  $\omega_0 = 62\,832\,000 \text{ Hz}$ .

Then on the basis of the value of  $\Delta X_L$  obtained at long times (6.56  $\Omega$ ) we calculate that the adsorption of GOx leads to a mass increase of 0.31  $\mu\text{g cm}^{-2}$ , equivalent to  $1.6 \times 10^{-12} \text{ mol cm}^{-2}$  based on a relative molar mass of 186 000 g mol<sup>-1</sup>. This can be compared with the expected value for a close packed monolayer of GOx of  $4.7 \times 10^{-12} \text{ mol cm}^{-2}$  based on the known dimensions of the molecule.<sup>8</sup>

(32) Molinero, V.; Calvo, E. J. Submitted for publication in *J. Electroanal. Chem.*

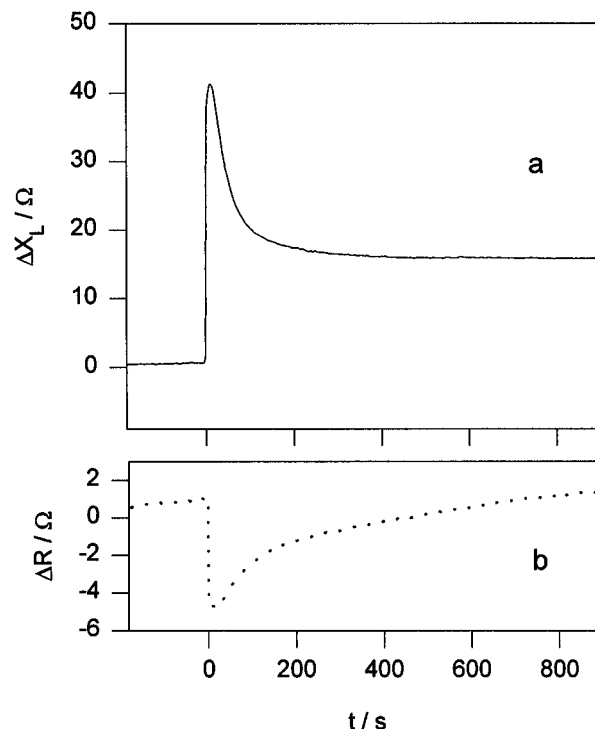


**Figure 6.** *In situ* quartz crystal impedance transients for the adsorption of GOx on Au/thiol/PAA-Fc (third GOx layer).

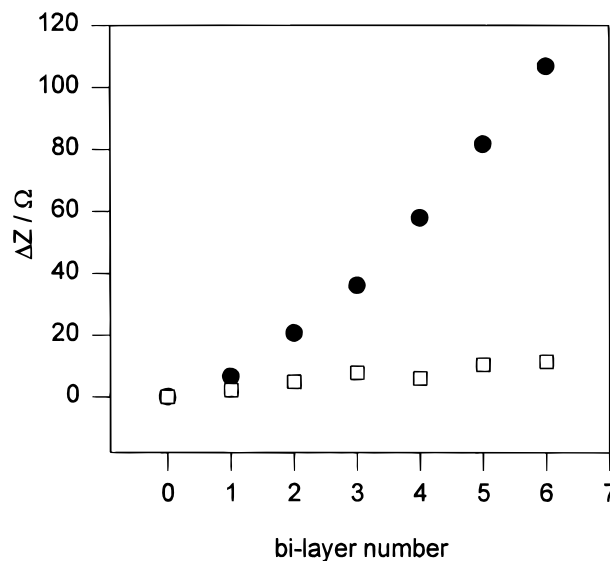


**Figure 7.** Change in quartz crystal impedance ((a) ●,  $\Delta X_L$ ; (b) □,  $\Delta R$ ) due to alternate PAA-Fc adsorbed bilayers.

**Multiple PAA-Fc/GOx Bilayers.** Having established that we can use the QCM to follow the deposition of the first layers of polymer and enzyme, we now go on to consider the deposition of multilayer structures. Multiple PAA-Fc/GOx bilayers can be deposited by alternate immersion of the thiol-modified Au electrode in polycationic ferrocene-modified poly(allylamine) solution and polyanionic glucose oxidase (GOx) solutions. This leads to the layer-by-layer construction of a bioelectrocatalytic structure.

Figure 7 depicts the change of steady state quartz impedance parameters,  $\Delta X_L$  and  $\Delta R$ , as a function of the number of PAA-Fc/GOx adsorbed bilayers for GOx-terminated layers. In all cases we note that  $\Delta R \ll \Delta X_L$  so that, to a good approximation, we can use eq 2 to obtain estimates of the mass from the measured values of  $\Delta X_L$ . We also note that  $\Delta R$  increases with increasing number

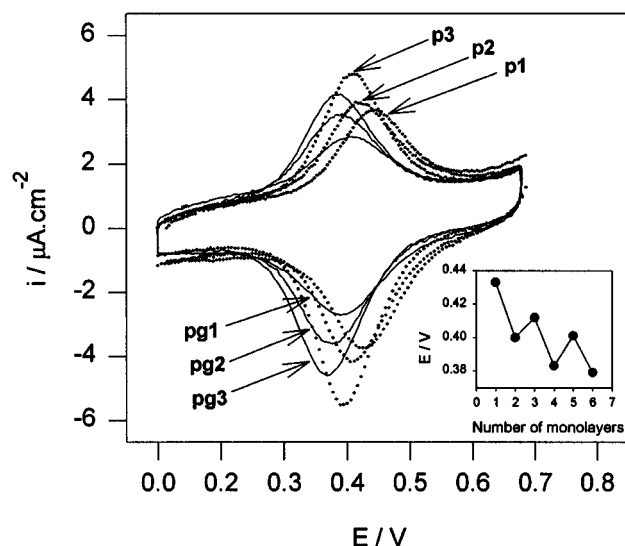


**Figure 8.** Cyclic voltammograms of self-assembled PAA-Fc/GOx multilayer in 10 mM acetate buffer of pH 5.0. P1, P2, and P3 correspond to polymer-terminated layers and PG1, PG2, and PG3 are GOx-terminated layers. Sweep rate was 50 mV s<sup>-1</sup>. Inset: Dependence of redox potential,  $E_{1/2}$ , on number of monolayers of the self-assembled multilayer PAA/GOx electrode.

of bilayers indicating, as expected, a slight increase in the viscoelastic resistance as the films become thicker. As described previously by Kunitake<sup>20b</sup> for GOx-PEI self-assembled layers, the mass changes for the first three bilayers are not constant (the areal mass increases by 0.30, 0.65, and then 0.70  $\mu\text{g cm}^{-2}$ , respectively). For four bilayers and above a linear increase of mass was observed for the subsequent addition of each polymer/GOx bilayer with a slope of  $24 \pm 0.7 \Omega$  corresponding to 1.1  $\mu\text{g cm}^{-2}$  of rigid mass increase for the addition of each successive bilayer. The contribution of adsorbed PAA-Fc to the total mass of each bilayer is less than 5%, so that most of the mass for each bilayer comes from the GOx. For the fourth and subsequent bilayers the loading of GOx in each bilayer is found to be  $5.9 \times 10^{-12} \text{ mol cm}^{-2}$ . This value is close to that calculated for a close packed monolayer and indicates that the PAA-Fc is effective in screening the electrostatic repulsion between the GOx molecules in the layer.

Kunitake *et al.*<sup>20b</sup> reported much larger surface concentrations of GOx adsorbed on polyethylenimine probably due to enzyme aggregation on the surface. We found that the kinetics of adsorption and the amount of enzyme adsorbed both strongly depend on the choice of experimental conditions, the enzyme purity, and concentration, solution pH, etc. These factors are being investigated at present.

Although the GOx dominates the QCM measurements because it makes up the main part of the mass of each bilayer, the buildup of ferrocene can be very easily followed in the electrochemistry. In all cases we find fast electron transfer from the underlying gold electrode to the successive ferrocene GOx bilayers as apparent from the small peak separation (Figure 8) and the linear dependence of the peak current on the potential sweep rate (see Figure 9). When we return to the variations in the electrochemistry as we build up the successive layers, we observe a number of interesting trends. First we note that there is a small decrease in the coverage of redox active ferrocene on adsorption of the GOx layer. This could arise either

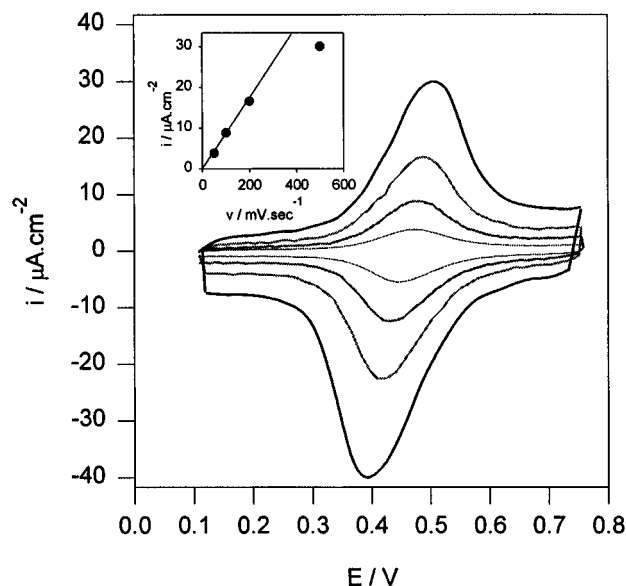


**Figure 9.** Cyclic voltammograms for an electrode with four PAA-Fc/GOx bilayers at different sweep rates: 50, 100, 200, 500 mV s<sup>-1</sup> in pH 5, 10 mM buffer. Inset: Dependence of the anodic peak current with potential sweep rate.

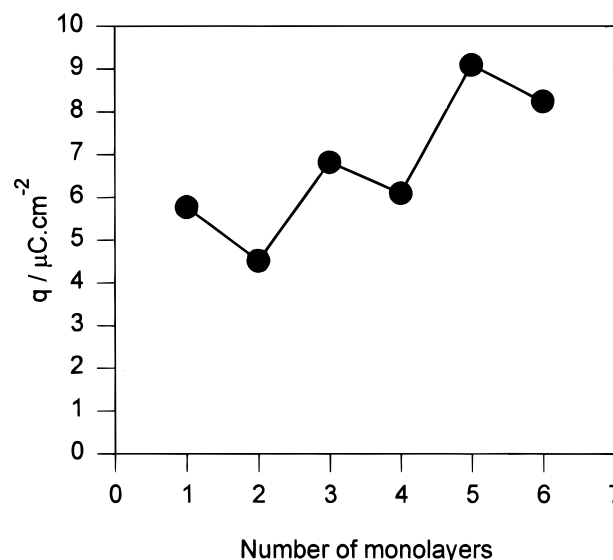
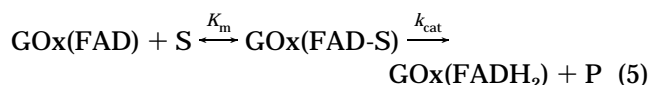
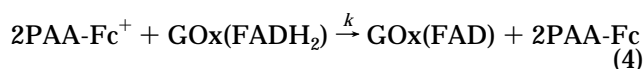
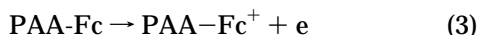


**Figure 10.** Dependence of integrated charge (●) of CV in Figure 8 for different monolayers of the self-assembled multilayer PAA-Fc/GOx electrode

through loss of PAA-Fc to the enzyme solution or through some of the ferrocene groups becoming non-redox active following adsorption of the enzyme onto the polymer. This effect can be seen in the charge data shown in Figure 10 where the total charge decreases by about 0.83  $\mu\text{C cm}^{-2}$  each time an outer GOx layer is added. However despite this effect there is a steady increase in the amount of redox active ferrocene on the electrode for each successive PAA-Fc GOx bilayer added. Second, we observe a systematic shift of the peak potential for the immobilized ferrocene back and forth as we build up the layers and as the outermost layer changes from PAA-Fc to GOx and back again; see the inset in Figure 8. Third, this systematic shift is accompanied by a variation in the full width at half height of the voltammograms. For the first PAA-Fc layer the peak is narrow (fwhh 106 mV), but on adsorption of GOx this broadens considerably (fwhh 131 mV). Addition of the next PAA-Fc layer results in a narrowing of the wave (fwhh 112 mV), and this trend continues as subsequent layers are added.

The negative shift of redox potential for anionic GOx-terminated layers suggests that the surface ferrocene is experiencing a different microenvironment from that within the film. The direction and magnitudes of the potential shifts are consistent with enhanced stabilization of the ferricinium ion by electrostatic interactions.<sup>33</sup> In a separate set of experiments using films of this type, we have found a negative shift of 36 mV per decade in the redox potential of the ferrocene as the concentration of the KNO<sub>3</sub> electrolyte is increased. Thus we postulate that there are at least two different ferrocene environments within the films and that this broadly explains the observed variations in the peak positions and peak width we find in the voltammetry.

**Glucose Oxidase Catalysis.** The oxidation of glucose catalyzed by glucose oxidase and mediated by the ferrocene-derivatized polymer can be described by the double redox–enzyme catalytic cycle<sup>3,4</sup>



where GOx(FADH<sub>2</sub>) and GOx(FAD) represent reduced and oxidized forms of glucose oxidase, PAA-Fc and PAA-Fc<sup>+</sup> the reduced and oxidized forms of the ferrocene redox polymer, and S and P are the substrate and product, β-D-glucose and glucono-D-lactone, respectively.

If we neglect diffusion of substrate for a thin enzyme layer, the expression for the catalytic glucose oxidation current density is<sup>10,13</sup>

$$I_{\text{cat}} = \frac{2F k_{\text{cat}} \Gamma_{\text{ET}}}{1 + \frac{k_{\text{cat}}}{k[\text{Fc}^+]} + \frac{K_m}{[\text{S}]}} \quad (6)$$

where Γ<sub>ET</sub> is the total enzyme surface concentration and [S] is the glucose concentration. The concentration of oxidized mediator in the polymer layer, [Fc<sup>+</sup>], depends on the electrode potential according to a modified Nernstian relation

$$[\text{Fc}^+] = [\text{Fc}_{\text{TOT}}] \frac{e^{(\beta F/RT)(E-E_{1/2})}}{1 + e^{(\beta F/RT)(E-E_{1/2})}} \quad (7)$$

where [Fc<sub>TOT</sub>] is the total volume concentration of ferrocene in the polymer layer, β is an interaction parameter which describes the broadening of the ferrocene redox wave by interactions within the film,<sup>3</sup> and E<sub>1/2</sub> is the half-wave potential of ferrocene in the polymer under these conditions. Figure 11 shows current–voltage curves for electrodes coated with one and four PAA-Fc GOx bilayers in a solution containing 50 mmol dm<sup>−3</sup> glucose. As the potential increases the ferrocene within the film is oxidized to ferricinium and we observe a catalytic current for the oxidation of glucose. This response is described by eqs 6 and 7, and the lines in Figure 11 correspond to the best fit of the data to these equations. For the single bilayer we find β = 0.59 and E<sub>1/2</sub> = 0.41 V, and for the four bilayer film β = 0.74 and E<sub>1/2</sub> = 0.40 V. It is satisfactory that the values of β and E<sub>1/2</sub> obtained from our analysis of the currents in the presence of glucose are consistent with

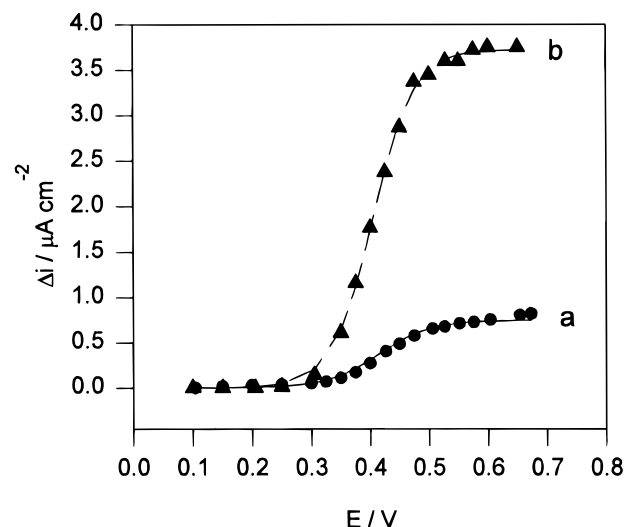


**Figure 11.** Dependence of steady state glucose catalytic oxidation current density on electrode potential for self-assembled PAA-Fc/GOx multilayer: (a) one bilayer, (b) four bilayers in 10 mM acetate buffer of pH 5.0 and 50 mM glucose after subtraction of background current. Solid line best fit line with eq 6 (see text).

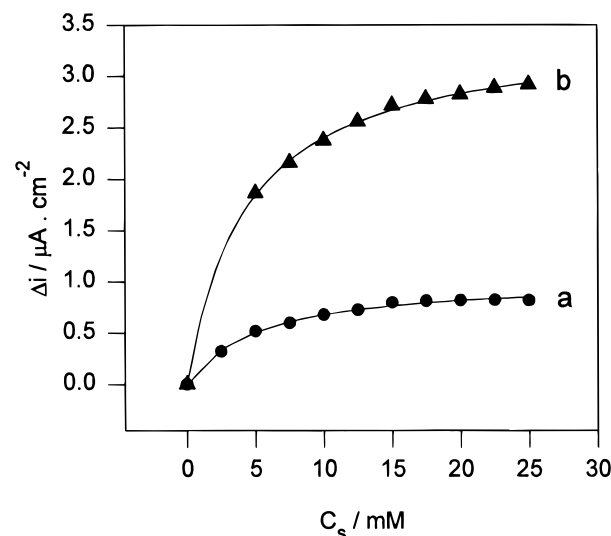


**Figure 12.** Glucose calibration curves of steady state catalytic current density as a function of glucose concentration for one PAA-Fc/GOx bilayer (●) and four bilayers (Δ). Solid line: best fit curve of data with eq 6, details given in the text. Background currents were subtracted.

the values we obtain from the voltammetry in glucose-free solution (β = 0.69, E<sub>1/2</sub> = 0.40 and β = 0.86, E<sub>1/2</sub> = 0.40 for the one and four bilayer films, respectively).

Figure 12 shows calibration curves for β-D-glucose oxidation at one and four ferrocene-polymer/GOx bilayer coated electrodes. The solid lines are the best fits of the data to eq 6, where we have replaced [Fc<sup>+</sup>] by [Fc<sub>TOT</sub>] because we are in the limiting current region. The resulting fitting parameters are given in Table 1. First we consider the values for K<sub>M</sub>/(1 + k<sub>cat</sub>/k[Fc<sub>TOT</sub>]). We note that these are approximately constant for the two films as expected. Substituting in estimates for K<sub>M</sub> and k<sub>cat</sub> of 25 mmol dm<sup>−3</sup> and 700 s<sup>−1</sup> from the literature<sup>34</sup> we obtain an estimate of k[Fc<sub>TOT</sub>] of 2000 s<sup>−1</sup>. Then, using the cyclic voltammetry data we can estimate [Fc<sub>TOT</sub>] from the charge passed and an estimate of the film thickness of 5.5 nm per

(33) Rowe, G. K.; Creager, S. E. *Langmuir* **1991**, 7, 2307–2312.

(34) Wilson, R.; Turner, A. P. F. *Biosens. Bioelectron.* **1992**, 7, 165–185.



**Table 1. Best Fit Parameters Obtained by Fitting the Data in Figure 12 to Equation 6**

no. of bilayers	$K_M/(1 + k_{\text{cat}}/k[\text{Fc}_{\text{TOT}}])/\text{mol cm}^{-3}$	$k_{\text{cat}}\Gamma_{\text{ET}}/K_M/\text{cm s}^{-1}$
1	$1.8 \times 10^{-5}$	$5.0 \times 10^{-7}$
4	$1.9 \times 10^{-5}$	$2.16 \times 10^{-6}$

bilayer. This gives a value for  $[\text{Fc}_{\text{TOT}}]$  of  $10^{-4} \text{ mol cm}^{-3}$  so that we obtain an estimate for  $k$  the rate constant for reaction between GOx and the ferricinium ion in the film, of  $2 \times 10^4 \text{ dm}^3 \text{ mol}^{-1} \text{ s}^{-1}$ . This value agrees well with values for homogeneous mediation by ferrocene.<sup>35</sup> Turning to the values for  $k_{\text{cat}}\Gamma_{\text{ET}}/K_M$  in Table 1 we note that on going from one to four bilayers this parameter increases 4-fold as expected. Substitution of values for  $K_M$  and  $k_{\text{cat}}$  from the literature gives an estimate for  $\Gamma_{\text{ET}}$  of  $10^{-14} \text{ mol cm}^{-2}$ . This is significantly less than the value for the coverage of  $1.6 \times 10^{-12} \text{ mol cm}^{-2}$  which we obtain from the analysis of the QCM data. This could be because a good fraction of the enzyme molecules on the surface are inactive or are not properly wired by the redox polymer due to conformational factors. In order to distinguish these two possibilities, we looked at the effect on the catalytic current of adding a soluble redox mediator to the solution. In all cases addition of  $1 \text{ mmol dm}^{-3}$  ferrocenesulfonate led to an increase in the catalytic current in the presence of  $50 \text{ mmol dm}^{-3}$  glucose of between 3- and 10-fold. This clearly shows that there are enzyme molecules within the film which are enzymatically active but which are not electrically wired to the redox polymer. Taking a value for  $k$  for ferrocenesulfonate<sup>36</sup> of  $9.5 \times 10^4 \text{ dm}^3 \text{ mol}^{-1} \text{ s}^{-1}$  and using eq 6, we find that in the best cases we obtain an estimate of the enzyme coverage per bilayer of  $2 \times 10^{-12} \text{ mol cm}^{-2}$ , which approaches the value we obtain from the QCM data.

Thus the picture which emerges from this analysis is that within the multilayer film a proportion of the GOx molecules are very efficiently wired by the PAA-Fc ( $k[\text{Fc}_{\text{TOT}}] > k_{\text{cat}}$ ) while a large proportion remain enzymatically active but are inaccessible to the polymer bound mediator. We speculate that this is because of conformational effects within the films and the requirement for optimal placement of the ferrocene mediator groups with respect to the enzyme active site. Further studies are in progress to investigate this effect.

(35) Bartlett, P. N.; Tebbutt, P.; Whitaker, R. G. *Prog. React. Kinet.* **1991**, *16*, 55–155.

(36) Liaudet, E.; Battaglini, F.; Calvo, E. J. *J. Electroanal. Chem.* **1990**, *293*, 55–68.

## Conclusions

In this work we have shown that we can use electrostatically driven adsorption of a redox polymer and an enzyme to buildup, layer by layer, electrocatalytically active enzyme/mediator structures. We have been able to follow this process by making mass measurements using the QCM and quartz crystal impedance analysis and by using electrochemical measurements to follow the deposition of the redox active mediator. We find that for the PAA-Fc GOx system there is very effective electrochemical communication between the successive layers. We have been able to analyze the catalytic responses as a function of the potential, the number of bilayers, and the substrate concentration. In this way we obtain estimates for the kinetics of the reactions occurring within the layers. We find that a proportion of the GOx molecules within each layer are very efficiently wired by the PAA-Fc ( $k[\text{Fc}_{\text{TOT}}] > k_{\text{cat}}$ ). However a significant proportion of the enzyme is unable to communicate with the PAA-Fc although it remains enzymatically active. Thus a key area of further study is to find out why this is and to overcome the problem.

Finally it is interesting to compare the integrated chemical system described here with the more common redox hydrogel system. Both can be constructed from the same components; for example, we have previously described a GOx PAA-Fc hydrogel system.<sup>3</sup> However in the latter case we have no control over the organization of the functional components within the structure. The layer-by-layer assembly described here introduces this element of control and allows us to construct active, thin layers. In these multilayer structures the reaction occurs throughout the layer in contrast to the case for the much thicker hydrogel system where only the inner layer is found to be active because of transport limitations within the gel.<sup>4</sup> By adopting a layer-by-layer assembly technique, we achieve much greater control over the structure and we are able to analyze the catalytic responses in terms of a simple kinetic model.

**Acknowledgment.** This work was supported by Fundacion Antorchas (Argentina) and British Council. K.S. thanks the BBSRC for a research studentship.

LA962014H